

Does Timeboost Reduce MEV-Related Spam? Theory and Evidence from Layer-2 Transactions

Agostino Capponi¹ and Brian Zhu¹

¹Columbia University

Abstract. Maximal extractable value opportunities often induce spam in Layer-2 blockchains: many identical transactions are submitted near simultaneously, most of which revert, wasting blockspace. We study *Timeboost*, a mechanism on Arbitrum that auctions a timestamp advantage, crucial under first-come first-served sequencing rules. We develop a game-theoretic model in which users choose the number of transaction copies to submit, and extend upon the baseline setting by modeling the Timeboost auction and subsequent transaction submission behavior. We show that Timeboost reduces spam and increases sequencer/DAO revenue in equilibrium relative to the baseline, transferring user payments from revert costs to auction bids. Empirically, we assemble mempool data from multiple Layer-2 networks, measuring spam via identical transactions submitted in narrow time intervals, and conduct an event study around Timeboost adoption on Arbitrum using other L2s as contemporaneous benchmarks. We find a decline in MEV-related spam and an increase in revenue on Arbitrum post-adoption, consistent with model predictions.

1 Introduction

Decentralized finance has been a cornerstone of the Ethereum ecosystem since early on, enabling services like trading and lending via smart contracts, and it is increasingly shifting to Layer-2 (L2) blockchains, called *rollups*, where trading volumes are steadily rising. This growth is driven by rollups' ability to execute most computation off-chain, reducing fees and improving efficiency, while still posting transaction batches and proofs to Ethereum, inheriting some of its security guarantees. As DeFi activity on rollups expands, so do incentives for maximal extractable value (MEV), i.e. profitable opportunities enabled by the ability to include transactions and order them, such as arbitrage and liquidations.

On L2 networks where throughput is higher, fees are lower, and sequencing policies are algorithmic (e.g. priority gas auction (PGA) or first-come first-served (FCFS)), MEV searchers may be more inclined to submit many copies of the same transaction, with the goal of having one exploit an opportunity and the others failing. Under PGAs, this is done by increasing the priority gas fee bid slightly on each copy; under FCFS, a user can spam to improve the chance that one of their transactions gets the earliest timestamp.

To address these challenges, the Arbitrum Foundation introduced *Timeboost*, a market mechanism that complements the FCFS policy with an *Express*

Lane auction. Every minute, a sealed-bid, second-price auction selects the Express Lane controller who can send transactions to the sequencer without delay, while other transactions are intentionally delayed. By aiming to capturing MEV-related rents through the auction and reducing incentives for spam and latency arms races, Timeboost aims to better align incentives and improve fairness.

In this paper, we provide a novel theoretical model of MEV-related spam under (i) just the FCFS sequencing rule and (ii) the FCFS sequencing rule with Timeboost. This is complemented with a novel cross-chain empirical analysis of testable model predictions. Our contributions can be described as follows.

First, we develop a model of MEV spam in which N arbitrageurs choose the number of transaction copies to submit. In the baseline model, FCFS-like competition leads each arbitrageur to submit multiple copies and yields a simple closed-form characterization of equilibrium. We then extend the model to include the Express Lane, where an auction is first held to determine Express Lane rights, before the auction winner and losers decide on their submissions. We show that Express Lane strictly reduces total transaction submission volume and brings more revenue to the sequencer/DAO relative to the baseline.

Second, we provide empirical evidence from transaction data that Timeboost reduces MEV-related spam on Arbitrum. Constructing a panel dataset using transaction-level data across multiple L2s and identifying bursts of MEV competition via transactions with identical calldata submitted within narrow time windows, we use a difference-in-differences design with Arbitrum as the treated network and other L2s as contemporaneous controls to estimate the causal effect of Timeboost adoption on spam intensity and revenue. We find that Timeboost adoption is associated with a statistically and economically significant decline in duplication-based spam on Arbitrum. When adding proceeds from the Timeboost auctions with reverted gas fees, we find a significant increase in revenue to accrues to the sequencer/DAO. Interestingly, time-boosted transactions revert at higher rates than their non-time-boosted counterparts, suggesting that auction winners may overestimate their time advantage. This is complemented with a within-Arbitrum analysis showing a similar result after controlling for market conditions such as gas fees and volume on decentralized exchanges.

Our theoretical and empirical results provide preliminary evidence that Timeboost is achieving some of its intended goals, and highlight it as an example of a mechanism that moves competition away from valuable blockspace.

Timeboost Details At the start of each round, it runs a sealed-bid, second-price auction with reserve price to pick a single “express lane controller,” the only actor allowed to submit transactions through a dedicated express-lane (remote procedure call) RPC endpoint. Everyone else submits through normal RPCs, but their transactions are delayed by 200 milliseconds.

The system has five main parts: bidders (who deposit funds and submit EIP-712 signed bids for a target round), an off-chain auctioneer (who aggregates bids and computes the winner and clearing price), an on-chain auction contract (which resolves the auction and collects payments), the sequencer (which mon-

itors the contract and validates express-lane submissions), and the express lane itself (through which the winner sends prioritized transactions). Each express-lane transaction must include round-specific metadata—such as the round number, chain ID, nonce, and a signature so the sequencer can verify authenticity and correct sequencing. Auction proceeds go to the Arbitrum DAO Treasury.

Related Literature Since the seminal work of [1], there is a rich body of literature on maximal extractable value (MEV), spanning measurement, market structure, and mitigation mechanisms. Studies include the emergence of private order flow and auction-based infrastructure (e.g. Flashbots [9]). Subsequent empirical work evaluates how private pools reshape who captures MEV and what centralization pressures emerge in practice [11].

Another line of research explores ordering policies and sequencer design. [2] initiate the study of *verifiable sequencing rules* and propose a concrete *Greedy Sequencing Rule* (GSR) [4]. Complementary approaches propose alternative objectives for within-block ordering—for example, CLVR targets reduced intra-block AMM price volatility [7]. Finally, protocol-level user protections such as revert protection, with recent work quantifying how revert protection increases equilibrium revenue and efficiency in PGAs [12].

The original design of Timeboost, introduced in [5], demonstrates how paying for a user-chosen time advantage can mitigate inefficient latency competition. Subsequent work studies Express Lane design: [3] studies optimal behavior for time-boosted arbitrageurs and discusses how AMMs might adapt to capture the MEV, and [6] evaluates the performance of Timeboost’s ahead-of-time auction by comparing bids with markouts, showing that bids are noisy predictors of short-horizon extracted value. [8] provides a large-scale empirical analysis of Timeboost, finding substantial revert rates in express-lane transactions and concentration among auction participants, but does not compare MEV-related spam before and after Timeboost’s deployment. Our paper complements this by providing a robust event study around the deployment, showing that despite revert rates in timeboosted transactions, which our model also predicts, the overall level of MEV-related spam decreased post-adoption.

2 Model

We model a competition for a common value MEV opportunity. A sequencer orders transactions according to a first-come, first-served (FCFS) rule applied to their *arrival timestamps*. There are $n \geq 2$ arbitrageurs indexed by $i \in \{1, \dots, n\}$. Exactly one arbitrageur can capture the opportunity of value $v > 0$ by being sequenced first with the proper transaction; all other copies revert (or equivalently, fail to capture the opportunity). Arbitrageurs can submit multiple copies of the same MEV-exploiting transaction, incurring a linear per-copy cost that represents the expected economic cost of failed attempts.

Each submitted transaction experiences a random delay before it is observed by the sequencer for inclusion. Formally, the timestamp is shifted by an i.i.d. de-

lay $\varepsilon \sim F$ (with density f), capturing network latency. Suppose that arbitrageur i submits k_i copies of the transaction. Then the effective arrival timestamp relevant under FCFS is the minimum of k_i i.i.d. draws from F :

$$X_i(k_i) := \min\{\varepsilon_{i1}, \dots, \varepsilon_{ik_i}\}.$$

Under FCFS, arbitrageur i captures the opportunity iff $X_i(k_i) \leq \min_{j \neq i} X_j(k_j)$. Intuitively, submitting more copies reduces the minimum delay and increases the chance of being first. We assume that a successful transaction costs $g \in (0, v)$ in gas fees, and reverted transactions must pay a fraction $r \in (0, 1)$ of the gas fees for a successful transactions.

For tractability, we assume that latency is exponential distributed: a single copy has a delay of $\varepsilon \sim \text{Exp}(\lambda)$ with rate $\lambda > 0$. Then we have that

$$X_i(k_i) \sim \text{Exp}(k_i \lambda).$$

In practice, k_i should be a nonnegative integer, but for tractability, we relax this and allow arbitrageurs to choose fractional amounts for the number of copies to send, expanding their action space to $k_i \in \mathbb{R}_+$. While this breaks the interpretation that $X_i(k_i)$ is the minimum of several i.i.d. draws from F , we still have that $X_i(k_i) \sim \text{Exp}(k_i \lambda)$. Arbitrageur i 's expected payoff is then

$$\begin{aligned} u_i(k_i; k_{-i}) &= (v - (1 - r)g) \cdot \Pr\left(X_i(k_i) \leq \min_{j \neq i} X_j(k_j)\right) - rgk_i \\ &:= V \cdot \Pr\left(X_i(k_i) \leq \min_{j \neq i} X_j(k_j)\right) - Ck_i \end{aligned}$$

where we reparameterize with $V = v - (1 - r)g$ and $C = rg$.¹ Under independent exponentially-distributed latency delays, the win probability simplifies to

$$\Pr\left(X_i(k_i) \leq \min_{j \neq i} X_j(k_j)\right) = \frac{k_i}{k_i + \sum_{j \neq i} k_j}.$$

We solve for symmetric pure-strategy Nash equilibria, which are characterized by the following result. Proofs are in the appendix.

Proposition 2.1. *There exists a unique symmetric pure-strategy Nash equilibrium where the number of copies submitted by each arbitrageur is*

$$k^* = \frac{n-1}{n^2} \cdot \frac{V}{C}.$$

From Proposition 2.1, we can compute important equilibrium quantities. Let K^* be the total number of transactions submitted in equilibrium. This represents

¹ Note that the cost accounting is done by adding the revert costs for all transactions plus an additional gas fee if the transaction is successful.

the level of spam in the sequencer mempool, since $(K^* - 1)$ of these transactions will revert, and has formula

$$K^* = nk^* = \frac{n-1}{n} \cdot \frac{V}{C}.$$

We can also compute an individual arbitrageur’s equilibrium utility u_i^* , and how the total value V is split between users, captured by the term W^* , and revenue R^* accrued by the sequencer/DAO from reverted gas fees:²

$$u_i^* = \frac{V}{n} - Ck^* = \frac{V}{n^2}, \quad W^* = nu_i^* = \frac{V}{n},$$

$$R^* = V - W^* = \frac{n-1}{n} \cdot V$$

These corollaries highlight the core inefficiency motivating Timeboost-style mechanisms: competition for being first under FCFS induces redundant transaction copies. In later sections we show how auctioning a time advantage changes the competitive margin, reducing K^* and reallocating surplus away from revert-driven waste and toward auction payments.

3 Timeboost Auction

3.1 Modified Model and Equilibrium

We now model the auction for control of the *Express Lane*, which provides a time advantage. In practice, all non-timeboosted transactions have their recorded timestamp artificially delayed by T while timeboosted transactions receive no additional delay.³ The Express Lane mechanism allocates a fixed time advantage $T > 0$ through a sealed-bid, second-price auction. Arbitrageur i now has the following action space.

1. **Auction:** Arbitrageur i submits a bid b_i . The highest bidder wins the express lane for this opportunity and pays the second-highest bid.
2. **Submission:** Arbitrageur i chooses the number of copies to send conditional on the auction outcome: $k_w^{(i)}$ if they win, and $k_l^{(i)}$ if they lose.

As in the baseline model, each submitted copy experiences an exponential idiosyncratic latency delay before it is observed by the sequencer. Let $X_w(k_w) \sim \text{Exp}(k_w\lambda)$ denote the winner’s earliest timestamp and $X_\ell^{(j)} \sim \text{Exp}(k_\ell\lambda)$ denote loser j ’s earliest timestamp, with being independent across arbitrageurs. Now,

² To be precise in the case of Arbitrum, gas fees not spend on posting block data to the Ethereum mainnet go to the Arbitrum DAO.

³ We also abstract away from the fact that Express Lane control lasts for a minute, and still focus on a single MEV opportunity for simplicity.

the winner's effective arrival time is $X_w - T$, while each loser's effective arrival time is still $X_\ell^{(j)}$. Therefore the winner succeeds if and only if

$$X_w - T \leq \min_j X_\ell^{(j)}.$$

Similarly, a particular loser j succeeds if and only if

$$X_\ell^{(j)} < \min_{-j} X_\ell^{(-j)} \text{ and } X_\ell^{(j)} \leq X_w - T.$$

Since this is now a sequential game, we look for symmetric subgame-perfect Nash equilibria in both the auction bids and conditional copies submitted. By backward induction, we condition the results of the auction and focus on the submission subgame. Using standard probability calculations, we can express the winner's expected payoff, excluding the auction payment, as

$$u_w(k_w; k_l^{(j)}) = V \left(1 - \frac{\sum_j k_l^{(j)}}{k_w + \sum_j k_l^{(j)}} \cdot \exp(-k_w \lambda T) \right) - C k_w$$

and a loser j 's expected payoff as

$$u_l^{(j)}(k_l^{(j)}; k_w, k_l^{(-j)}) = V \left(\frac{k_l^{(j)}}{k_w + k_l^{(j)} + \sum_{-j} k_l^{(-j)}} \cdot \exp(-k_w \lambda T) \right) - C k_l^{(j)}.$$

The following result characterizes the submission subgame.

Proposition 3.1. *There exists a unique symmetric pure-strategy Nash equilibrium (k_l^*, k_w^*) in the submission subgame where k_l^* and k_w^* are the number of copies submitted by each arbitrageur conditional on losing and winning the auction, respectively, and satisfy $0 < k_l^* < k_w^*$. Moreover, letting u_l^* and u_w^* denote loser and winner payoffs in this equilibrium, we have $0 < u_l^* < u_w^*$.*

How an auctioned time advantage reshapes the FCFS spamming race is illustrated in Proposition 3.1. The ordering $0 < k_l^* < k_w^*$ captures the key behavioral response. Conditional on winning, an arbitrageur optimally submits more copies because each marginal copy is amplified by the time advantage, increasing the probability of being sequenced first; conditional on losing, the same trader scales back because additional copies compete under a systematic disadvantage.

Both roles earn a positive continuation payoff: even conditional on losing, an arbitrageur retains a positive chance of success (e.g. when the winner's minimum latency is not sufficiently small), so the optimal loser strategy yields a positive expected payoff. However, the auction winner enjoys a higher continuation surplus because the head start raises its success probability at any fixed intensity, and this advantage is not fully dissipated by quantity adjustment. This payoff gap is what supports a willingness to pay for the Express Lane and underpins the auction stage: equilibrium bids are ultimately tied to the incremental value from winning $u_w^* - u_l^*$, allowing the mechanism to extract surplus from latency races while preserving participation incentives.

Proposition 3.2. *Let $b^* = u_w^* - u_l^*$. Then (b^*, k_l^*, k_w^*) comprise the unique symmetric subgame-perfect Nash equilibrium in the full auction-submission sequential game.*

Proposition 3.2 ties everything together by showing that the unique equilibrium of the submission stage endogenously pins down a unique equilibrium of the preceding auction. In the sealed-bid second-price auction, bidding this value is the (unique symmetric) best response: any lower common bid can be profitably outbid to secure strictly positive surplus, while any higher common bid yields negative expected surplus relative to losing. As a result, $b^* = u_w^* - u_l^*$ is the unique symmetric equilibrium bid, and combining it with the submission strategies (k_l^*, k_w^*) yields a unique symmetric SPNE of the full sequential game.

3.2 Comparison with Baseline Setting

We now evaluate the same important quantities under Timeboost. The total number of transactions submitted in Timeboost equilibrium, denoted K_{tb}^* , is

$$K_{tb}^* = k_w^* + (n - 1)k_l^*.$$

Since the winner pays $u_w^* - u_l^*$ in Timeboost equilibrium, all arbitrageurs receive a equilibrium payoff of u_l^* . The division of the surplus value V between arbitrageurs and sequencer,⁴ denoted by components W_{tb}^* and R_{tb}^* , respectively, is

$$W_{tb}^* = nu_l^*, \quad R_{tb}^* = V - W_{tb}^* = V - nu_l^*.$$

Proposition 3.3. *Arbitrageurs send fewer total transactions and the sequencer earns more revenue in equilibrium under Timeboost than in the baseline setting, i.e. $K_{tb}^* < K^*$ and $R_{tb}^* > R^*$.*

The key mempool efficiency and revenue implications of Timeboost are summarized in Proposition 3.3. Relative to the baseline FCFS race, Timeboost reshapes the margin of competition away from spamming to purchasing an artificial ordering advantage. In equilibrium, this reduces the number submissions required to compete for the same opportunity: the winner and losers scale back because they obtain a systematic advantage or face a systematic disadvantage. Interpreting reverted copies as wasted blockspace, this captures a concrete efficiency gain, freeing up blockspace from failed race attempts.

The increase in revenue follows from the fact that Timeboost converts part of what would otherwise be dissipated in revert-related costs into direct payments to the sequencer. Even when revert costs are collected by the sequencer, the key revenue channel in Timeboost comes from changing (i) the type of time advantage provided and (ii) how it is priced. Instead of submitting more copies to marginally improve the best timestamp, Timeboost offers a substantial, guaranteed time advantage that can be viewed as a highly desirable “premium” product. Additionally, by selling that advantage via a second-price auction, arbitrageurs are incentivized to bid their true value for it, i.e. the added value from winning, thus allowing the auctioneer to fully extract this value.

⁴ Similarly to gas fees, Timeboost auction proceeds go to the Arbitrum DAO.

4 Data

We assemble a panel of on-chain activity for Arbitrum and a set of major EVM L2 comparison networks using Dune Analytics. We collect data from the Arbitrum, Optimism, Polygon, Base, and Avalanche (C-Chain) blockchains between February 17 and June 17 of 2025, a two-month window before and after the deployment of Timeboost, which happened on April 17, 2025. Our objective is to measure spamming and wasteful competition among bots and searchers. This phenomenon is relevant both in FCFS sequencer settings, where arrival timing drives inclusion, and PGA environments, where actors repeatedly submit or adjust transactions to win priority.

To measure spamming in a comparable way across chains, we look for bursts of near-identical transactions within short second-level windows. Setting a window length of 2 seconds, we track the transaction’s sender, recipient, value, function selector, and calldata. If transactions with these same characteristics appear multiple times in the same burst window, we label all transactions beyond the first as repeated (redundant) attempts, interpreting them as a conservative proxy for automated resubmission and competitive duplication. This is motivated by common bot execution logic: when inclusion and ordering are uncertain, whether due to FCFS latency dispersion, PGA-style priority competition, or optimistic MEV transactions [10].

We first record the number of repeated transactions and the gas consumed by failed repeated transactions, denoted by $\text{RepTXs}_{c,t}$ and $\text{RepGas}_{c,t}$, where c indexes a blockchain and t indexes the time period. We additionally record failed repeated transactions $\text{FailedRepeatedTXs}_{c,t}$ and the percentage failure rate among these repeated transactions, given by

$$\text{PctFailed}_{c,t} = \frac{\text{FailedRepeatedTXs}_{c,t}}{\text{RepTXs}_{c,t}}$$

capturing futile attempts consistent with losing races or reacting too slowly to state changes. For the purposes of our empirical analysis, on Arbitrum, we compute $\text{PctFailed}_{c,t}$ using only non-timeboosted transactions (while $\text{RepTXs}_{c,t}$ and $\text{RepGas}_{c,t}$ are still computed using all transactions).

On Arbitrum after the implementation of Timeboost, the auction proceeds also contribute to the revenue. We thus collect data for each Timeboost auction round within our sample window, focusing on the payment, denoted by AuctionPayment_t , of the winner (the second-highest bid). Letting the $\text{Revenue}_{c,t}$ variable integrating revenue from gas fees and auctions across Layer 2s:

$$\text{Revenue}_{c,t} = \text{RepGas}_{c,t} + \text{AuctionPayment}_t \cdot 1_{\{c=\text{Arbitrum}\}}.$$

We collect a set of controls, including base gas fees and DEX volume on each blockchain, as well as returns and volatility of Ether (relative to US dollars). While Arbitrum, Optimism, and Base use ETH for gas payments, Polygon and Avalanche use native tokens; to account for this, we convert values into ETH. All variables are aggregated at daily frequencies.

Chain	RepTXs				Revenue				PctFailed			
	Mean	SD	Min	Max	Mean	SD	Min	Max	Mean	SD	Min	Max
Arbitrum	68,416	92,305	2,850	643,983	57.14	78.64	0.322	592.3	30.5	18.5	0.8	82.1
Avalanche	2,774	4,625	304	39,127	0.026	0.046	0.001	0.262	19.0	18.4	0.4	95.7
Base	216,987	142,519	62,578	857,769	0.503	0.879	0.108	8.215	20.2	15.4	0.2	64.5
Optimism	43,092	56,968	2,701	516,531	0.012	0.017	0.002	0.156	2.0	5.5	0.0	36.0
Polygon	11,290	7,686	2,577	36,718	0.001	0.002	0.000	0.009	27.0	11.8	3.1	67.0

Table 1: Summary statistics by chain for total repeated transactions, sequencer revenue, and the percentage of repeated transactions that fail.

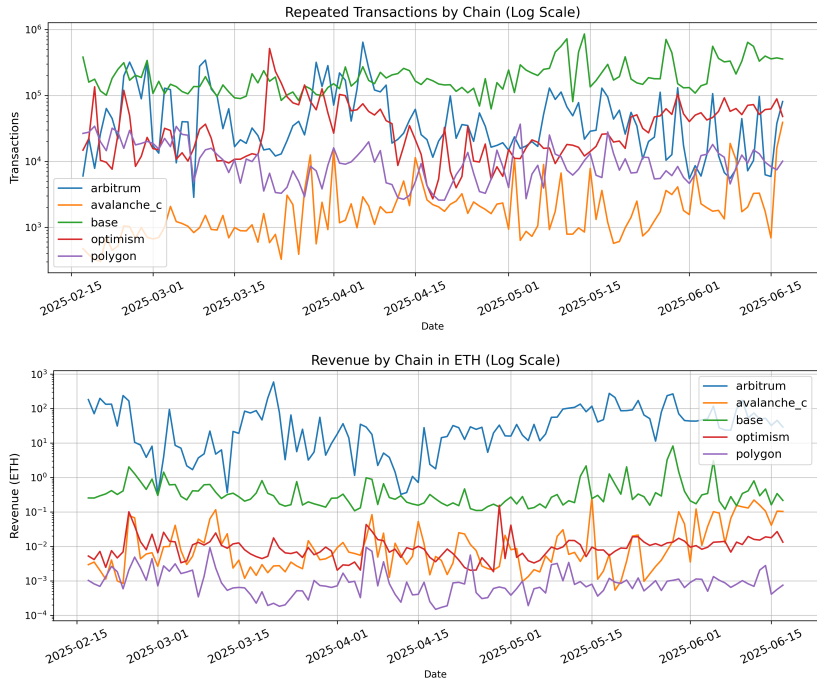


Fig. 1: Top: Repeated transactions across chains. Bottom: Revenue in ETH from reverted transactions and auction proceeds for Arbitrum after April 17 (log scales).

Summary statistics in Table 1 show substantial heterogeneity across chains in all three metrics of interest. Base and Arbitrum exhibit the highest average repeated transaction counts, indicating more activity and frequent competition over MEV, while Polygon and Avalanche are far lower in levels. Failure rates also differ markedly: Arbitrum and Polygon have relatively high mean failure rates while Optimism stands out with a much lower mean failure share. Revenue varies by orders of magnitude as well, as Arbitrum’s mean is far larger than the other chains, likely due to higher base gas fees and the magnitude of transactions processed. Time series for these metrics are shown in Figures 1 and 2.

Figure 2 highlights an interesting phenomenon where timeboosted repeated transactions fail at higher rates than non-timeboosted repeated transactions, a notable departure from our model, which predicts that Express Lane controllers win more and scale back the number of copies submitted due to the time advantage. One explanation for this, drawing on the work of [8], is that the low number of participants in the auction (usually between Wintermute, Selini Capital, and Kairos addresses) does not provide large variation in winners, and that these winners may overestimate the advantage that Timeboost provides.

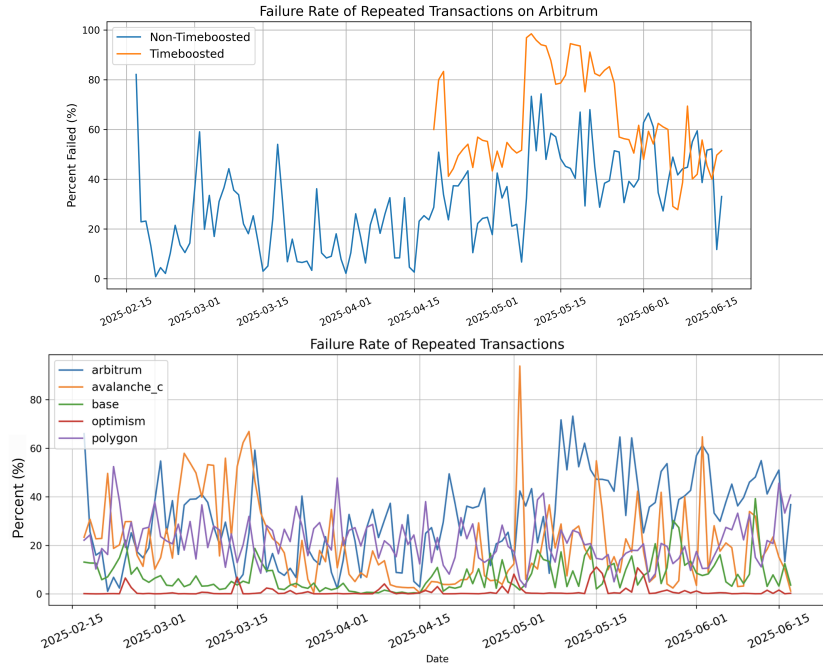


Fig. 2: Top: Percentage of repeated transactions that failed on Arbitrum, separated by timeboosted status. Bottom: Percentage of repeated transactions that failed on L2s.

5 Empirical Analysis

In this section, we provide an empirical analysis of Timeboost on transaction spamming in Arbitrum. There are three testable implications of our model:

1. Timeboost decreases transaction spamming. (Proposition 3.3)
2. Timeboost increases sequencer/DAO revenue. (Proposition 3.3)
3. Disadvantaged users win less often, thus having their transactions fail more often under Timeboost. (Follows from $k_l^* < k_w^*$ in Proposition 3.1)

To test these implications, we conduct a panel data analysis using data across Layer 2 blockchains and a within-Arbitrum analysis.

5.1 Across Layer 2s

We estimate the causal effect of Timeboost on transaction spamming, sequencer revenue, and non-timeboosted failure rate using a difference-in-differences (DiD) design that compares changes on Arbitrum (the treated chain) before and after the Timeboost launch to contemporaneous changes on a set of comparison L2 networks with no major changes to their sequencer ordering rules. The identifying variation is thus cross-sectional (treated vs. control chains) interacted with time-series variation (post- vs. pre-implementation). We supplement the baseline specification with controls for fee conditions and market intensity, respectively: an L2 base fee measure in Ether (**BaseGasL2**) and within-chain DEX volume in log USD as a DeFi activity proxy (**VolumeDEX**).

All outcome variables and time-varying covariates (except for the binary treatment indicator) are standardized (z-scored) prior to estimation. This choice is practical and methodological: chains differ by orders of magnitude in baseline transaction counts, gas usage, and revenue, and raw-unit levels can cause the regression to be dominated by the largest networks, conflating scale with treatment response. Standardization produces estimates in standard-deviation units, improving comparability across chains and outcomes and making effect sizes interpretable on a common scale. Importantly, standardization does not change the sign or statistical significance patterns relative to monotone transformations.

Empirical Specification and Identification. Formally, our specification is given by the following model:

$$Y_{c,t} = \beta \cdot \text{Post} \times \text{Treated}_{c,t} + \gamma^\top X_{c,t} + \alpha_c + \delta_t + \varepsilon_{c,t}$$

where the dependent variable of interest (repeated transactions or revenue) is

$$Y \in \{\log \text{RepTXs}, \log \text{Revenue}, \text{PctFailed}\},$$

$\text{Post} \times \text{Treated}_{c,t} = 1_{\{c=\text{Arbitrum}, t \geq 2025-04-17\}}$ denotes the treatment effect (i.e. the differential change on Arbitrum after Timeboost relative to the change on control chains over the same period),

$$X \subseteq \{\text{BaseGasL2}, \text{VolumeDEX}\}$$

is a set of controls, and $\varepsilon_{c,t}$ is idiosyncratic noise. We include chain fixed effects α_c that absorb time-invariant differences across networks (e.g., average activity levels, application mix, sequencer infrastructure) and day fixed effects δ_t that absorb common shocks shared across chains (e.g., market-wide volatility, macro crypto news, broad changes in user demand).

A key DiD identification assumption is parallel trends conditional on fixed effects and controls: absent Timeboost, would Arbitrum’s outcomes have behaved similarly to the control L2s, after conditioning on fixed effects and control variables? From Figure 1, this assumption is visually supported by the random-looking pre-trends, with high chain-specific volatility and occasional correlations

around market trends. We empirically probe this assumption by designating alternate dates before the actual deployment day as the treatment date (shown in the appendix). The assumption also relies on the control L2s having no sequencing rule shocks, which to the authors’ knowledge, holds for the time window.⁵

TABLE 5.1	(1)	(2)	(3)	(4)	(5)	(6)
	log RepTXs	log RepTXs	log Revenue	log Revenue	PctFailed	PctFailed
Post×Treated	-0.699** (0.281)	-0.698*** (0.254)	0.726*** (0.123)	0.711*** (0.112)	0.968*** (0.235)	0.956*** (0.241)
BaseGasL2		0.096 (0.076)		0.150** (0.071)		0.115** (0.045)
VolumeDEX		0.159 (0.125)		0.078 (0.150)		0.052 (0.070)
Observations	605	605	605	605	605	605
N. of groups	5	5	5	5	5	5
R ²	0.025	0.041	0.001	0.032	0.083	0.096

Includes chain and day fixed effects. Standard errors are clustered by chain.

Note:

*p<0.1; **p<0.05; ***p<0.01

Discussion of Results. Table 5.1 reports difference-in-differences estimates of the effect of Timeboost adoption on repeated transaction activity, revenue, and failure rate. The coefficient on `Post×Treated` is negative and statistically significant (about -0.70 standard deviations), indicating that after Timeboost implementation, Arbitrum experienced a sizable decline in repeated transactions relative to the comparison L2s. This estimate is nearly unchanged when adding controls, suggesting that this reduction is not merely driven by coincident changes in transaction costs or market-wide trading activity.

The `PostTreated` coefficient for revenue is positive and significant, implying that after Timeboost, revenue from reverted transactions and gas fees increased overall. Finally, the `PostTreated` coefficients for failure rate of non-timeboosted transactions is positive and significant, demonstrating a marked disadvantage for arbitrageurs without time advantages.

In the appendix, we provide additional robustness checks: we vary the window of measuring repeated transactions from 2 seconds to 5 seconds, and change the duration of the window before and after the Timeboost adoption date. These results carry through, with the decline in repeated transactions and gain in revenue after Timeboost adoption being significant across these changes.

5.2 Within Arbitrum

Our cross-chain DiD design controlled variation across chains and time by introducing fixed effects. Now, we complement the analysis with a within-Arbitrum

⁵ Note the Base adopted Flashblocks on July 7, 2025.

analysis by directly incorporating variables that would potentially influence transaction volumes. This exercise does not replace the DiD identification strategy, as it lacks an external control group, but provides a useful additional robustness check: if Timeboost meaningfully altered submission behavior, we should observe significant changes on Arbitrum itself, particularly after conditioning on proxies for activity (DEX volume) and transaction costs (L1 and L2 base fees).

Empirical Specification. We estimate an model of the form

$$Y_t = \alpha + \beta \cdot \text{Post}_t + \gamma^\top X_t + \varepsilon_t \quad (1)$$

where the dependent variable of interest is

$$Y \in \{\log \text{RepTXs}, \log \text{Revenue}, \text{PctFailed}\},$$

$\text{Post}_t = 1_{\{t \geq 2025-04-17\}}$ is a post-implementation indicator, and

$$X \subseteq \{\text{VolumeDEX}, \text{BaseGasMain}, \text{BaseGasArb}, \text{VolatilityETH}\}$$

is a vector of time-varying controls. In all specifications we include a measure of DEX volume and base gas fees on Ethereum; we additionally include Arbitrum base gas fee and ETH volatility to capture additional shifts in arbitrage intensity. As a robustness check (reported in the appendix), we also verify that conclusions are not sensitive to alternative bandwidths around the implementation date and alternative time intervals for short-window repetition. Here, we do *not* standardize variables before estimation.

Discussion of Results. Table 5.2 reports the within-Arbitrum estimates. The post-Timeboost indicator is negative and statistically significant for RepTXs, implying a sizable decrease in repeated submissions after the implementation date even after controlling for DEX volume and fee conditions; the point estimate remains similar when adding mainnet base fees and market controls. Similarly to the cross-chain analysis, there is a positive significant relation between the post-Timeboost period and revenue, and the post-Timeboost period is associated with higher failure rates among non-timeboosted transactions.

DEX volume is positively related to repeated transactions, consistent with higher trading activity increasing the number of contested opportunities and associated transaction flow. The coefficient on BaseGasArb is large and positive in the repeated transactions regressions, which is expected as Arbitrum gas fees are determined by congestion and would be higher under more spammed transactions. The coefficients on BaseGasMain and BaseGasArb for the revenue regressions tell a more interesting story: revenue from reverted gas fees and auction proceeds appears to be driven by base gas on Ethereum, with Arbitrum gas fees and volatility having a second-order effect. Taken together, the within-chain estimates provide complementary evidence that Timeboost’s implementation is associated with a reduction in repeated submissions on Arbitrum.

TABLE 5.2	(1)	(2)	(3)	(4)	(5)	(6)
	log RepTXs	log RepTXs	log Revenue	log Revenue	PctFailed	PctFailed
Intercept	-9.423 (5.991)	-8.955 (6.110)	2.621 (7.327)	-4.377 (7.449)	-0.971 (0.702)	-0.845 (0.764)
Post	-0.578** (0.238)	-0.453* (0.240)	0.858** (0.354)	0.594* (0.360)	0.179*** (0.033)	0.182*** (0.037)
VolumeDEX	1.004*** (0.299)	0.882*** (0.312)	-0.026 (0.364)	0.427 (0.382)	0.056 (0.035)	0.049 (0.040)
BaseGasMain	-0.050 (0.158)	-0.146 (0.155)	0.631*** (0.189)	0.690*** (0.198)	0.051** (0.022)	0.051** (0.023)
BaseGasArb		187.350*** (54.911)		-94.886* (50.138)		-0.206 (6.754)
VolatilityETH		0.262 (0.768)		-3.216*** (0.846)		0.057 (0.104)
Observations	121	121	121	121	121	121
R^2	0.173	0.257	0.068	0.141	0.412	0.415
Adjusted R^2	0.152	0.218	0.044	0.096	0.397	0.385

Standard errors are computed using the Newey-West estimator.

Note: *p<0.1; **p<0.05; ***p<0.01

6 Conclusion

TimeBoost changes transaction ordering on Arbitrum by introducing a distinct express lane for time-sensitive activity. Our theoretical framework clarifies why such a mechanism can reduce wasteful competition: when actors can purchase a time advantage through an explicit allocation mechanism rather than racing in the public queue, the equilibrium incentive to submit redundant copies falls and surplus is more likely to be captured through payments rather than dissipated in spam, freeing up blockspace.

Empirically, we test these findings using complementary cross-chain and within-Arbitrum designs. The cross-chain difference-in-differences results show a large, robust post-adoption decline in repeated transaction activity on Arbitrum relative to other L2s, consistent with reduced redundant competition. The results also show an increase in revenue from gas fees and auction proceeds, suggesting that TimeBoost is able to capture more of the MEV via its auction. Failure rates of non-timeboosted MEV-related transactions increased post-adoption, illustrating the effects of the time disadvantage incurred by those who did not win the auction. The within-Arbitrum analysis yields similar results.

Future work can extend the theory by considering heterogeneous latencies and strategic participation, or dive deeper into the reasons why overall revenue does not increase and why timeboosted transactions fail more often than their non-timeboosted counterparts. Overall, our theoretical framework and empirical shows that TimeBoost meaningfully reshapes competition for MEV opportunities and can resolve spam-related inefficiencies in Layer 2 networks.

References

1. Philip Daian, Steven Goldfeder, Tyler Kell, Yunqi Li, Xueyuan Zhao, Iddo Bentov, Lorenz Breidenbach, and Ari Juels. Flash boys 2.0: Frontrunning, transaction reordering, and consensus instability in decentralized exchanges, 2019. Also appears as an IEEE S&P 2020 paper. [arXiv:1904.05234](https://arxiv.org/abs/1904.05234), [doi:10.48550/arXiv.1904.05234](https://doi.org/10.48550/arXiv.1904.05234).
2. Matheus V. X. Ferreira and David C. Parkes. Credible decentralized exchange design via verifiable sequencing rules. In *Proceedings of the 55th Annual ACM Symposium on Theory of Computing (STOC 2023)*, pages 723–736, 2023. [doi:10.1145/3564246.3585233](https://doi.org/10.1145/3564246.3585233).
3. Robin Fritsch, Maria Inês Silva, Akaki Mamageishvili, Benjamin Livshits, and Edward W. Felten. Mev capture through time-advantaged arbitrage, October 2024. URL: <https://arxiv.org/abs/2410.10797>, [arXiv:2410.10797](https://arxiv.org/abs/2410.10797).
4. Yuhao Li, Mengqian Zhang, Jichen Li, Elynn Chen, Xi Chen, and Xiaotie Deng. Mev makes everyone happy under greedy sequencing rule, 2023. ACM CCS Workshop on Decentralized Finance and Security (DeFi’23). [arXiv:2309.12640](https://arxiv.org/abs/2309.12640), [doi:10.48550/arXiv.2309.12640](https://doi.org/10.48550/arXiv.2309.12640).
5. Akaki Mamageishvili, Mahimna Kelkar, Jan Christoph Schlegel, and Edward W. Felten. Buying time: Latency racing vs. bidding in transaction ordering, June 2023. URL: <https://arxiv.org/abs/2306.02179>, [arXiv:2306.02179](https://arxiv.org/abs/2306.02179).
6. Akaki Mamageishvili, Christoph Schlegel, Sunghun Ko, Jinsuk Park, and Ali Taslimi. Timeboost: Do ahead-of-time auctions work?, November 2025. URL: <https://arxiv.org/abs/2511.18328>, [arXiv:2511.18328](https://arxiv.org/abs/2511.18328).
7. Robert McLaughlin, Nir Chemaya, Dingyue Liu, and Dahlia Malkhi. Clvr ordering of transactions on amms, 2025. [arXiv:2408.02634](https://arxiv.org/abs/2408.02634), [doi:10.48550/arXiv.2408.02634](https://doi.org/10.48550/arXiv.2408.02634).
8. Johnnatan Messiah and Christof Ferreira Torres. The express lane to spam and centralization: An empirical analysis of arbitrum’s timeboost, September 2025. URL: <https://arxiv.org/abs/2509.22143>, [arXiv:2509.22143](https://arxiv.org/abs/2509.22143).
9. Alex Obadia. Flashbots—frontrunning the mev crisis. <https://writings.flashbots.net/frontrunning-mev-crisis>, 2020. Accessed 2025-12-03.
10. Ozan Solmaz, Lioba Heimbach, Yann Vonlanthen, and Roger Wattenhofer. Optimistic mev in ethereum layer 2s: Why blockspace is always in demand. In *7th Conference on Advances in Financial Technologies (AFT 2025)*, 2025. [doi:10.4230/LIPIcs.AFT.2025.28](https://doi.org/10.4230/LIPIcs.AFT.2025.28).
11. Ben Weintraub, Christof Ferreira Torres, Cristina Nita-Rotaru, and Radu State. A flash(bot) in the pan: Measuring maximal extractable value in private pools. In *Proceedings of the 22nd ACM Internet Measurement Conference (IMC ’22)*, 2022. [doi:10.1145/3517745.3561448](https://doi.org/10.1145/3517745.3561448).
12. Brian Z. Zhu, Xin Wan, Ciamac C. Moallemi, Dan Robinson, and Brad Bachu. Quantifying the value of revert protection, 2025. Originally submitted Oct 2024; revised Feb 2025. [arXiv:2410.19106](https://arxiv.org/abs/2410.19106), [doi:10.48550/arXiv.2410.19106](https://doi.org/10.48550/arXiv.2410.19106).

A Proofs

A.1 Proof of Proposition 2.1

Differentiating the arbitrageur's objective with respect to k_i gives

$$\frac{\partial u_i}{\partial k_i} = V \cdot \frac{k_{-i}}{(k_i + k_{-i})^2} - C.$$

Note that for fixed k_{-i} , $\partial u_i / \partial k_i$ is positive at k_i and decreases monotonically to $-C$ in k_i , so there exists a unique interior maximum. Imposing symmetry, we have $k_i = k^*$ for all i . The first-order condition is then

$$V \cdot \frac{(n-1)k^*}{(nk^*)^2} = C.$$

Solving for k^* yields the result.

A.2 Proof of Proposition 3.1

Let $K_L := \sum_{j \neq w} k_i^{(j)}$ denote total loser intensity, and for a fixed loser $i \neq w$ define

$$B_i := k_w + \sum_{\substack{j \neq w \\ j \neq i}} k_i^{(j)},$$

the total intensity of all agents other than i once w is fixed.

Lemma 1. Fix $k_w \geq 0$ and $\{k_i^{(j)}\}_{j \neq w, i}$, hence fixing $B_i > 0$ and $A := Ve^{-k_w \lambda T} > 0$. Then the loser payoff

$$u_i^L(k) = A \frac{k}{k + B_i} - Ck \quad (k \geq 0)$$

is strictly concave in k .

Proof. Differentiate:

$$\frac{d}{dk} \left(\frac{k}{k + B_i} \right) = \frac{B_i}{(k + B_i)^2}, \quad \frac{d^2}{dk^2} \left(\frac{k}{k + B_i} \right) = -\frac{2B_i}{(k + B_i)^3} < 0.$$

Thus $A \frac{k}{k + B_i}$ is strictly concave and subtracting Ck preserves strict concavity. Therefore u_i^L is strictly concave on $[0, \infty)$ and admits at most one maximizer. Since $u_i^L(k) \rightarrow -\infty$ as $k \rightarrow \infty$ and u_i^L is continuous, a maximizer exists.

Lemma 2. Fix $\{k_i^{(j)}\}_j$, hence K_L . Then the winner payoff $u_w(k) := u_w(k; K_L)$ is strictly concave in k on $[0, \infty)$, hence has a unique maximizer $k_w^{w, \text{BR}}$.

Proof. If $K_L = 0$, then $P_w \equiv 1$ and $u_w(k) = V - Ck$ is maximized uniquely at $k = 0$. Assume $K_L > 0$ and set $a := \lambda T > 0$. Write

$$u_w(k) = V - Vh(k) - Ck, \quad h(k) := \frac{K_L e^{-ak}}{k + K_L}.$$

A direct calculation gives

$$h''(k) = \frac{K_L (a^2(k + K_L)^2 + 2a(k + K_L) + 2) e^{-ak}}{(k + K_L)^3} > 0 \quad \text{for all } k \geq 0,$$

so h is strictly convex. Hence $-Vh(k) - Ck$ is strictly concave, i.e. u_w is strictly concave on $[0, \infty)$. Moreover $u_w(k) \leq V - Ck \rightarrow -\infty$ as $k \rightarrow \infty$, so a maximizer exists, and strict concavity implies it is unique.

Together, the lemmas show that for any fixed profile of opponents' intensities, each player has a unique optimal choice in the relevant role. We now restrict attention to symmetric profiles in the submission subgame: the winner uses k_w and every loser uses the same k_l . Define

$$D := k_w + (n - 1)k_l.$$

Under symmetry, the winner's and a representative loser's payoffs are

$$\begin{aligned} u_w(k_w, k_l) &= V \left(1 - \frac{(n-1)k_l}{D} e^{-k_w \lambda T} \right) - Ck_w, \\ u_l(k_w, k_l) &= V \left(\frac{k_l}{D} e^{-k_w \lambda T} \right) - Ck_l. \end{aligned}$$

The symmetric interior best responses satisfy the first-order conditions

$$0 = \frac{\partial u_w}{\partial k_w} = \left(\frac{(n-1)k_l}{D^2} + \frac{(n-1)k_l}{D} \lambda T \right) e^{-k_w \lambda T} V - C, \quad (2)$$

$$0 = \frac{\partial u_l}{\partial k_l} = \left(\frac{k_w + (n-2)k_l}{D^2} \right) e^{-k_w \lambda T} V - C. \quad (3)$$

Let (k_l, k_w) be any interior solution and define the dimensionless variable

$$x := (n-1)k_l \lambda T.$$

Divide (2) by (3) to eliminate the common factor $e^{-k_w \lambda T} V / C$:

$$\frac{(n-1)k_l}{D^2} + \frac{(n-1)k_l}{D} \lambda T = \frac{k_w + (n-2)k_l}{D^2}.$$

Multiplying by D^2 and simplifying gives

$$k_w - k_l = (n-1)k_l \lambda T \cdot D. \quad (4)$$

Write $r := k_w / k_l$ and note $D = k_l(r + n - 1)$. Substituting into (4) and using $x = (n-1)k_l \lambda T$ yields

$$r - 1 = x(r + n - 1).$$

Solving for r gives

$$\frac{k_w}{k_l} = r(x) := \frac{1 + (n-1)x}{1-x}. \quad (5)$$

In particular, $k_w > 0$ implies $1-x > 0$, so any interior solution must satisfy $x \in (0, 1)$. Substitute (11) into the loser FOC (3) to obtain a single equation in x . Using

$$k_l = \frac{x}{(n-1)\lambda T}, \quad k_w = r(x)k_l, \quad D = k_w + (n-1)k_l = \frac{nk_l}{1-x},$$

and noting that

$$k_w \lambda T = r(x) k_l \lambda T = r(x) \frac{x}{n-1} =: a(x) = \frac{x(1+(n-1)x)}{(n-1)(1-x)},$$

the loser FOC (3) becomes

$$(n-1)\lambda T H(x) = \frac{R}{V}, \quad x \in (0, 1), \quad (6)$$

where

$$H(x) := \frac{(n-1+x)(1-x)}{xn^2} e^{-a(x)}.$$

We now show that (6) has a unique solution $x^* \in (0, 1)$. Consider $\log H(x)$:

$$\log H(x) = \log(n-1+x) + \log(1-x) - \log x - a(x) - 2 \log n.$$

Differentiating,

$$\frac{d}{dx} \log H(x) = \frac{1}{n-1+x} - \frac{1}{1-x} - \frac{1}{x} - a'(x).$$

A direct calculation shows $a'(x) > 0$ on $(0, 1)$, hence for $x \in (0, 1)$ and $n \geq 2$

$$\frac{d}{dx} \log H(x) < \frac{1}{n-1+x} - \frac{1}{1-x} - \frac{1}{x} \leq \frac{1}{n-1} - \left(\frac{1}{x} + \frac{1}{1-x} \right) < 0$$

because $\frac{1}{x} + \frac{1}{1-x} \geq 4$ for all $x \in (0, 1)$. Therefore H is strictly decreasing on $(0, 1)$. Finally, we check boundary limits. As $x \downarrow 0$,

$$H(x) \sim \frac{n-1}{n^2} \cdot \frac{1}{x} \rightarrow +\infty,$$

and as $x \uparrow 1$, we have $1-x \rightarrow 0$ and $a(x) \rightarrow +\infty$, hence $e^{-a(x)} \rightarrow 0$ and $H(x) \rightarrow 0$. Since H is continuous and strictly decreasing, (6) has a unique solution $x^* \in (0, 1)$.

Given x^* , the corresponding (k_l^*, k_w^*) are uniquely recovered by

$$k_l^* = \frac{x^*}{(n-1)\lambda T}, \quad k_w^* = r(x^*) k_l^*,$$

and (11) ensures the winner FOC (2) is also satisfied whenever (3) is. This proves uniqueness. From (11), for any interior solution $x \in (0, 1)$,

$$\frac{k_w^*}{k_l^*} = r(x) = \frac{1 + (n-1)x}{1-x} > 1,$$

since the numerator exceeds 1 and the denominator is in $(0, 1)$. Hence $k_w^* > k_l^*$.

In an interior equilibrium with $k_l^* > 0$ and $k_w^* > 0$, let $D^* := k_w^* + (n-1)k_l^*$. Using the loser FOC to substitute for R , we obtain

$$u_l^* = e^{-k_w^* \lambda T} V \left(\frac{k_l^*}{D^*} \right)^2 > 0.$$

Since k_w^* is a best response given k_l^* ,

$$u_w^* = \max_{k \geq 0} u_w(k, k_l^*) \geq u_w(k_l^*, k_l^*).$$

Moreover, $u_l(k_w, k_l^*)$ is strictly decreasing in k_w , and $k_w^* > k_l^*$, so

$$u_l^* = u_l(k_w^*, k_l^*) < u_l(k_l^*, k_l^*).$$

Therefore,

$$u_w^* - u_l^* > u_w(k_l^*, k_l^*) - u_l(k_l^*, k_l^*) = V(1 - e^{-k_l^* \lambda T}) > 0,$$

which implies $u_w^* > u_l^*$.

A.3 Proof of Proposition 3.2

Let $n \geq 2$ bidders participate in a sealed-bid second-price auction and

$$v_A := u_w^* - u_l^*$$

denote each bidder's (common, known) incremental value of winning the Express Lane right, i.e. the difference between being the winner and being a loser in the continuation game. Conditional on the submission-subgame equilibrium being played after the auction, a bidder who wins and pays price p obtains utility $u_w^* - p$, while a bidder who loses obtains utility u_l^* . Thus the incremental gain from winning at price p is $v_A - p$.

Consider a symmetric pure bid profile in which all bidders submit the same bid $b \geq 0$. Under uniform tie-breaking, each bidder wins with probability $1/n$ and pays the (second-highest) price b whenever they win. Hence each bidder's expected utility is

$$U(b) = \frac{1}{n}(u_w^* - b) + \frac{n-1}{n}u_l^* = u_l^* + \frac{1}{n}(v_A - b). \quad (7)$$

Fix such a symmetric profile and consider a unilateral deviation by bidder i :

1. If $b < v_A$, bidder i can deviate to $b + \varepsilon$ for any sufficiently small $\varepsilon > 0$. Then bidder i wins with probability 1 and pays the second-highest bid, which remains b . The deviation payoff is therefore $u_w^* - b = u_l^* + (v_A - b)$, which strictly exceeds $U(b) = u_l^* + (v_A - b)/n$ because $v_A - b > 0$ and $n \geq 2$. Hence no symmetric profile with $b < v_A$ can be a Nash equilibrium.
2. If $b > v_A$, bidder i can deviate to a sufficiently low bid (e.g. 0), guaranteeing that they lose and obtain u_l^* . Under the symmetric profile, their payoff is $U(b) = u_l^* + (v_A - b)/n < u_l^*$. Thus any symmetric profile with $b > v_A$ admits a profitable deviation and cannot be a Nash equilibrium.
3. If $b = v_A$, then $U(v_A) = u_l^*$. Deviating to any bid $b_i < v_A$ guarantees losing and yields u_l^* , which equals $U(v_A)$. Deviating to any bid $b_i > v_A$ guarantees winning and paying v_A , yielding $u_w^* - v_A = u_l^*$, again equal to $U(v_A)$. Therefore no deviation yields a strictly higher payoff, so $b = v_A$ is a best response to the symmetric profile.

Combining (1)–(3), it follows that the only symmetric pure bid profile that can be a Nash equilibrium is $b^* = v_A$, and it is indeed a Nash equilibrium. We proceed to verify sequential rationality in every subgame.

1. From Proposition 3.1, after any realized auction winner, the continuation strategies form a Nash equilibrium of the corresponding submission subgame. Hence no player can profitably deviate after observing the auction outcome.
2. Given that the continuation equilibrium is played after the auction, each bidder's value for winning the Express Lane right is $v_A = u_w^* - u_l^*$. By the previous proposition, bidding $b^* = v_A$ is a best response (indeed, the unique symmetric pure-strategy equilibrium bid) to the others bidding b^* . Therefore no bidder can profitably deviate in the auction stage.

Thus, the overall strategy profile is subgame-perfect.

A.4 Proof of Proposition 3.3

Less Transaction Spamming. In the Express Lane submission subgame, let the winner choose k_w and each of the $n - 1$ losers choose k_l , and define $D := k_w + (n - 1)k_l$. The symmetric interior first-order conditions are

$$\left(\frac{(n-1)k_l}{D^2} + \frac{(n-1)k_l}{D} \lambda T \right) e^{-k_w \lambda T} V = C, \quad (8)$$

$$\left(\frac{k_w + (n-2)k_l}{D^2} \right) e^{-k_w \lambda T} V = C. \quad (9)$$

Dividing (8) by (9) eliminates the common factor $e^{-k_w \lambda T} V$ and yields

$$\frac{(n-1)k_l}{D^2} + \frac{(n-1)k_l}{D} \lambda T = \frac{k_w + (n-2)k_l}{D^2}.$$

Multiplying by D^2 and rearranging gives the identity

$$k_w - k_l = (n-1)k_l \lambda T \cdot D. \quad (10)$$

Define the dimensionless variable

$$x := (n-1)k_l\lambda T.$$

From (10), any interior solution has $x \in (0, 1)$ and

$$\frac{k_w}{k_l} = r(x) := \frac{1 + (n-1)x}{1-x}. \quad (11)$$

Consequently,

$$N_{tb}^*(T) = D = k_w + (n-1)k_l = k_l(r(x) + n-1) = \frac{nk_l}{1-x} = \frac{nx}{(n-1)\lambda T(1-x)}. \quad (12)$$

Moreover,

$$k_w\lambda T = r(x)k_l\lambda T = r(x)\frac{x}{n-1} =: a(x) = \frac{x(1+(n-1)x)}{(n-1)(1-x)}. \quad (13)$$

Substitute (11)–(13) into the loser FOC (9). Using $D = \frac{nk_l}{1-x}$, $e^{-k_w\lambda T} = e^{-a(x)}$, and $k_w + (n-2)k_l = k_l\frac{n-1+x}{1-x}$, we obtain

$$\frac{V}{C} = \frac{n^2x}{(n-1)\lambda T(n-1+x)(1-x)} e^{a(x)}. \quad (14)$$

Therefore baseline total intensity can be expressed as

$$N_{\text{base}}^* = \frac{n-1}{n} \frac{V}{C} = \frac{nx}{\lambda T(n-1+x)(1-x)} e^{a(x)}. \quad (15)$$

Taking the ratio of (12) and (15) yields

$$\frac{N_{tb}^*(T)}{N_{\text{base}}^*} = \frac{n-1+x}{n-1} e^{-a(x)} = \left(1 + \frac{x}{n-1}\right) e^{-a(x)}. \quad (16)$$

Since $x \in (0, 1)$, (13) implies

$$a(x) = \frac{x}{n-1} \cdot \frac{1+(n-1)x}{1-x} > \frac{x}{n-1}. \quad (17)$$

Using the inequality $\log(1+y) < y$ for all $y > 0$ with $y = x/(n-1)$, we have

$$\log\left(1 + \frac{x}{n-1}\right) < \frac{x}{n-1} < a(x).$$

Exponentiating gives $1 + \frac{x}{n-1} < e^{a(x)}$, hence $\left(1 + \frac{x}{n-1}\right) e^{-a(x)} < 1$. By (16),

$$\frac{N_{tb}^*(T)}{N_{\text{base}}^*} < 1,$$

which implies $N_{tb}^*(T) < N_{\text{base}}^*$ for all $T > 0$.

More Sequencer Revenue. From our derived formulas for sequencer revenue in both the baseline setting and under Timeboost, this reduces to showing $u_l^* < V/n^2$ for any $T > 0$.

Let $D^* := k_w^* + (n-1)k_l^*$ denote total intensity in the Express Lane equilibrium. Using the loser first-order condition (9) to substitute for R in the loser payoff yields the identity

$$u_l^* = e^{-k_w^* \lambda T} V \left(\frac{k_l^*}{D^*} \right)^2. \quad (18)$$

Moreover, since $k_w^* > k_l^*$ when $T > 0$, hence $D^* = k_w^* + (n-1)k_l^* > nk_l^*$ and therefore $(k_l^*/D^*)^2 < 1/n^2$. Since $e^{-k_w^* \lambda T} < 1$ for $T > 0$ and $k_w^* > 0$, (18) yields

$$u_l^* = e^{-k_w^* \lambda T} V \left(\frac{k_l^*}{D^*} \right)^2 < V \cdot \frac{1}{n^2}.$$

Thus $u_l^* < V/n^2$, which implies the result.

B Robustness Checks

B.1 Prior Treatment Date as Placebo

For a properly identified DiD setup, significant treatment effects should disappear when designating a date before the actual treatment date. We move the “treatment date” 15 days earlier to April 2, 2025.

	(1)	(2)	(3)	(4)	(5)	(6)
	log RepTXs	log RepTXs	log Revenue	log Revenue	PctFailed	PctFailed
Post×Treated	-0.318 (0.314)	-0.347 (0.294)	0.213 (0.144)	0.158 (0.131)	0.885*** (0.214)	0.846*** (0.239)
BaseGasL2		0.097 (0.071)		0.153** (0.069)		0.106** (0.053)
VolumeDEX		0.167 (0.121)		0.069 (0.160)		0.010 (0.064)
Observations	605	605	605	605	605	605
N. of groups	5	5	5	5	5	5
R^2	0.005	0.023	0.003	0.033	0.064	0.075

Includes chain and day fixed effects. Standard errors are clustered by chain.

Note:

*p<0.1; **p<0.05; ***p<0.01

B.2 Narrower Study Window

We narrow the study window by 15 days on both ends, so that the new sample period is from March 2 to June 2, 2025.

	(1)	(2)	(3)	(4)	(5)	(6)
	log RepTXs	log RepTXs	log Revenue	log Revenue	PctFailed	PctFailed
Post×Treated	-0.564** (0.242)	-0.587** (0.238)	0.964*** (0.044)	0.924*** (0.052)	0.901*** (0.332)	0.839*** (0.354)
BaseGasL2		0.059 (0.050)		0.104 (0.067)		0.134* (0.080)
VolumeDEX		0.058 (0.091)		0.132 (0.149)		0.053 (0.094)
Observations	465	465	465	465	465	465
N. of groups	5	5	5	5	5	5
R^2	0.016	0.020	0.060	0.081	0.066	0.090

Includes chain and day fixed effects. Standard errors are clustered by chain.

Note: *p<0.1; **p<0.05; ***p<0.01

Table 5.2	(1)	(2)	(3)	(4)	(5)	(6)
	log RepTXs	log RepTXs	log Revenue	log Revenue	PctFailed	PctFailed
Intercept	-11.000* (5.681)	-11.939* (6.153)	-3.732 (6.958)	-8.377 (7.223)	-0.496 (0.748)	-0.329 (0.858)
Post	-0.462* (0.259)	-0.390 (0.263)	1.307*** (0.355)	1.155*** (0.370)	0.177*** (0.030)	0.185*** (0.032)
VolumeDEX	1.090*** (0.283)	1.053*** (0.315)	0.286 (0.345)	0.563 (0.366)	0.033 (0.038)	0.021 (0.045)
BaseGasMain	-0.200 (0.149)	-0.264* (0.145)	0.355** (0.169)	0.376** (0.175)	0.063*** (0.022)	0.060*** (0.022)
BaseGasArb		169.113*** (52.415)		-19.931 (34.822)		4.831 (7.640)
VolatilityETH		-0.114 (0.839)		-1.926** (0.775)		0.076 (0.102)
Observations	123	123	123	123	123	123
R^2	0.224	0.255	0.313	0.342	0.410	0.414
Adjusted R^2	0.205	0.224	0.296	0.314	0.396	0.389

Standard errors are computed using the Newey-West estimator.

Note: *p<0.1; **p<0.05; ***p<0.01

B.3 Wider Interval for Repeated Transactions

We widen the interval under which we search for repeated transactions from 2 seconds to 5 seconds.

Table 5.2	(1)	(2)	(3)	(4)	(5)	(6)
	log RepTXs	log RepTXs	log Revenue	log Revenue	PctFailed	PctFailed
Post	-0.671*** (0.191)	-0.673*** (0.159)	0.772*** (0.195)	0.724*** (0.135)	1.007*** (0.268)	0.993*** (0.278)
BaseGasL2		0.145*** (0.044)		0.403*** (0.115)		0.115*** (0.037)
VolumeDEX		0.207* (0.108)		0.139 (0.128)		0.037 (0.052)
Observations	605	605	605	605	605	605
N. of groups	5	5	5	5	5	5
R^2	0.022	0.056	0.033	0.204	0.126	0.138

Includes chain and day fixed effects. Standard errors are clustered by chain.

Note: *p<0.1; **p<0.05; ***p<0.01

Table 5.2	(1)	(2)	(3)	(4)	(5)	(6)
	log RepTXs	log RepTXs	log Revenue	log Revenue	PctFailed	PctFailed
Intercept	-9.453 (5.784)	-9.028 (5.859)	0.566 (7.011)	-6.362 (7.060)	-1.175* (0.652)	-1.053 (0.704)
Post	-0.542** (0.228)	-0.416* (0.228)	0.783** (0.344)	0.527 (0.350)	0.152*** (0.030)	0.158*** (0.034)
VolumeDEX	1.015*** (0.288)	0.894*** (0.299)	0.084 (0.348)	0.529 (0.360)	0.068** (0.033)	0.059 (0.036)
BaseGasMain	-0.062 (0.152)	-0.159 (0.149)	0.608*** (0.182)	0.663*** (0.191)	0.047** (0.020)	0.045** (0.021)
BaseGasArb		190.117*** (52.041)		-86.322* (50.565)		4.105 (6.421)
VolatilityETH		0.243 (0.723)		-3.182*** (0.830)		0.056 (0.088)
Observations	121	121	121	121	121	121
R^2	0.262	0.315	0.229	0.313	0.398	0.401
Adjusted R^2	0.243	0.285	0.209	0.283	0.383	0.375

Standard errors are computed using the Newey-West estimator.

Note: *p<0.1; **p<0.05; ***p<0.01